Biochim Biophys Acta. Author manuscript; available in PMC 2016 August 31.

Published in final edited form as:
Biochim Biophys Acta. 2011 October ; 1808(10): 2359–2365. doi:10.1016/j.bbamem.2011.06.016.

Instability of toxin A subunit of AB_5 toxins in the bacterial periplasm caused by deficiency of their cognate B subunits

Sang-Hyun Kim[a], **Su Hyang Ryu**[a], **Sang-Ho Lee**[a], **Yong-Hoon Lee**[a], **Sang-Rae Lee**[a], **Jae-Won Huh**[a], **Sun-Uk Kim**[a], **Ekyune Kim**[d], **Sunghyun Kim**[b], **Sangyong Jon**[b], **Russell E. Bishop**[c,*], and **Kyu-Tae Chang**[a,**]

[a]The National Primate Research Center, Korea Research Institute of Bioscience and Biotechnology (KRIBB), Ochang, Cheongwon, Chungbuk 363–883, Republic of Korea

[b]School of Life Science, Gwangju Institute of Science and Technology (GIST), 1 Oryong-dong, Gwangju 500–712, Republic of Korea

[c]Department of Biochemistry and Biomedical Sciences, McMaster University, Hamilton, Ontario, Canada L8N 3Z5

[d]College of Pharmacy, Catholic University of Daegu, Hayang-eup, Gyeongsan, Gyeongbuk 712-702, Republic of Korea

Abstract

Shiga toxin (STx) belongs to the AB_5 toxin family and is transiently localized in the periplasm before secretion into the extracellular milieu. While producing outer membrane vesicles (OMVs) containing only A subunit of the toxin (STxA), we created specific STx1B- and STx2B-deficient mutants of *E. coli* O157:H7. Surprisingly, STxA subunit was absent in the OMVs and periplasm of the STxB-deficient mutants. In parallel, the A subunit of heat-labile toxin (LT) of enterotoxigenic *E. coli* (ETEC) was absent in the periplasm of the LT-B-deficient mutant, suggesting that instability of toxin A subunit in the absence of the B subunit is a common phenomenon in the AB_5 bacterial toxins. Moreover, STx2A was barely detectable in the periplasm of *E. coli* JM109 when *stx2A* was overexpressed alone, while it was stably present when *stxB* was co-expressed. Compared with STx2 holotoxin, purified STx2A was degraded rapidly by periplasmic proteases when assessed for in vitro proteolytic susceptibility, suggesting that the B subunit contributes to stability of the toxin A subunit in the periplasm. We propose a novel role for toxin B subunits of AB_5 toxins in protection of the A subunit from proteolysis during holotoxin assembly in the periplasm.

Keywords

Shiga toxin; Heat-labile toxin; Outer membrane; Periplasm; *Escherichia coli*

*Corresponding author. Tel.: +1 905 525 9140x28810; fax: +1 905 522 9033. **Corresponding author. Tel.: +82 43 240 6300; fax: +82 43 240 6309.

1. Introduction

Shiga toxin (STx) elaborated by *E. coli* O157:H7 is a typical AB_5 exotoxin consisting of an A subunit and five identical B subunits [1–3]. The catalytic A subunit of STx (STxA; ~32 kDa protein) shows a ribosomal RNA (rRNA) *N*-glycosidase activity that specifically cleaves a conserved adenine base of 28S rRNA of the 60S ribosomal subunit, which eventually blocks protein synthesis and causes cell death [4]. The STxB subunit (~7.7 kDa protein) binds specifically to the host cell membrane-anchored globotriaosylceramide (Gb3) receptor [5], thereby mediating subsequent internalization of the toxin [3]. In the absence of STxA, STxB can associate in a ring-like pentameric structure in the periplasm and can be substantially entrapped into OMVs for extracellular secretion [6,7]. In general, STx toxins can be classified into two types: STx1 (also known as VT1 for verotoxin or SLT-I for Shiga-like toxin) and STx2 (also known as VT2 or SLT-II). STx1 is nearly identical to the Shiga toxin of *Shigella dysenteriae* serotype 1, differing only by one amino acid (AA), but shares overall 56% identity with the AA sequence of STx2 types [1,8]. The Sakai strain of *E. coli* O157:H7 is capable of producing both STx1 and STx2, which are encoded by *stx1* and *stx2* operons (*stx1AB* and *stx2AB*), respectively [8]. STxs are believed to play a key role in the pathogenesis of hemolytic uremic syndrome (HUS) [9]. However, effective prevention and therapeutic interventions against the O157 infection and its sequela HUS are yet to be developed.

Heat-labile toxin (LT) of enterotoxigenic *E. coli* (ETEC), the causative agent of traveler's diarrhea, also belongs to the AB_5 toxin family. Like STx, LT, encoded by a two-gene operon (*lt-AB*), is exported in a Sec-dependent manner to the periplasm where holotoxin assembly occurs with one catalytic A subunit (LT-A; ~28 kDa) and a homopentamer of B subunits (LT-B; 11.6 kDa) [10,11]. Extracellular export of LT across the outer membrane (OM) takes place via a specific type II secretion system (T2SS) encoded by a gene cluster comprising *gspC* to *gspM* [11]. However, no specific T2SS has been identified for the extracellular secretion of STx from Shiga toxin-producing *E. coli* (STEC). Thus, OMVs are likely utilized as non-specific extracellular secretion vehicles for exporting STx accumulated in the periplasm of STEC lacking the specialized toxin secretion system [12,13]. Consistently, STx holotoxins and STxB pentamers were known to be largely enclosed within OMVs [7,14]. Although LT is secreted by the specific T2SS, approximately 95% of LT is still associated with the OMV because the extracellular LT is able to bind to sugar residues in lipopolysaccharide (LPS) on the surface of ETEC [15,16].

In our previous reports [7,17], we genetically detoxified the OMVs of O157 *E. coli* with the aim of generating low-endotoxic and STxA-deficient OMVs that could be useful as vaccine vehicles. Next, we tried to produce OMVs of O157 *E. coli* containing STxA uncoupled with STxB by creating an internal deletion in the *stxB* gene. However, we found that the STxA could hardly exist as a free form in the periplasm, which prevents secretion of the free A subunit via OMVs. Collectively, in this study, we have shown that periplasmic expression and subsequent extracellular secretion of STxA-subunit alone is impossible without assistance by STxB. Our findings reveal a novel role for the B subunit in stabilizing the A subunit during AB_5 toxin assembly in the periplasm. A chaperone-like role for the toxin B subunit in the periplasm is thus proposed.

2. Materials and methods

Bacterial strains and plasmids used in this study are listed in Table 1.

2.1. Creation of stx and degP mutants of E. coli O157:H7

E. coli O157:H7 strain Sakai [8] and its derivative Sakai-DM [17] possessing less-endotoxic LPS (due to lack of MsbB myristoylation in lipid A biosynthesis) were used as parental strains for creation of site-specific mutations by using an allelic exchange procedure assisted by the Red recombinase carried in pKD46, as described previously [7,17,18]. In addition to pKD46, plasmid pKD3 was used commonly for construction of mutated alleles containing the chloramphenicol (Cm)-cassette and pCP20 was used for excision of the Cm-cassette from the resulting chromosomal mutant [18]. Transformants were plated in Luria-Bertani (LB) agar, containing the appropriate antibiotics (Cm: 20 μg/ml, ampicillin (Amp): 100 μg/ml), and potential mutants were confirmed by a genomic PCR and DNA sequence analysis.

As *E. coli* O157:H7 Sakai strain possesses two *stx* operons, single Δ*stx1B* or Δ*stx2B* mutant and the combined Δ*stx1B*/Δ*stx2B* double mutant were created with targeting DNA template constructed in pUC18-based recombinant plasmids pSTx1B::Cm and pSTx2B::Cm (Table 1). Construction of those template plasmids (pSTx1B::Cm and pSTx2B::Cm) was started by cloning of intact DNA fragments containing *stx1B* and *stx2B* genes, then an inverse PCR was conducted to remove internal 180-bp DNA fragments from each ORF. The primers for inverse PCR are as follows; the forward primer (Fw1B-Kpn): CTGTCATAAT*GGTACC*GGGATTCAGCGAAG and the reverse primer (Re1B-Sal): TCAGGC*GTCGAC*AGCGCACTTGCTG for *stx1B*, and the forward primer (Fw2B-SacI): CCTGTGAATCA*GAGCTC*CGGATTTGCT and the reverse primer (Re2B-Sal): GCACAATCC*GTCGAC*ATTGCATTAACAG for *stx2B*, respectively. To incorporate the Cm-cassette (from pKD3) into the deleted DNA regions of the two *stxB* ORFs, the inverse PCR products were digested with restriction enzymes recognizingtheprimer sequence underlined, then the Cm-cassette DNA was inserted into the *stxB* alleles.

Similarly, an inverse PCR strategy was employed for construction of Δ*degP*::Cm allele in pUC18-based pDegP::Cm vector, with a view to creating WT/Δ*stx2B*/Δ*degP*::Cm mutant (Table 1). The inverse PCR was conducted with a primer set; the forward (Deg-SalF): CGGGTGAT-GT*GTCGAC*CTCACTGAAC and the reverse (Deg-KpnR): GACCAAA-CGG*GGTACC*AATCGCTAC. Then, the Cm-cassette was inserted into the *Sal*I-*Kpn*I sites generated by the inverse PCR primers underlined.

2.2. Creation of Δlt-B::Cm mutant of ETEC H10407

An allelic exchange approach was employed to make a mutation in the chromosome of ETEC H10407 carrying pKD46, by using the mutated allele constructed in the template plasmid. Construction of the Δ*lt-B*::Cm allele was started by cloning of DNA fragment (~834-bp) for the region of *lt-AB* operon. Then, an inverse PCR was carried out with primers of LTB-BamF (CTATCATATAC*GGATCC*GATGGCAGG) and LTB-SalR (GAGAGGATA*GTCGAC*GCCGTAAATAA) to delete internal 120-bp DNA and to generate the restriction enzyme sites incorporated in the primers underlined. The Cm-cassette DNA

digested with *Sal*I-*Bam*HI at both ends was then inserted into the deleted region of the *lt-B* allele. Subsequently, the Δ*lt-B*::Cm allele was introduced into ETEC H10407 carrying pKD46 by electroporation to create the Δ*lt-B*::Cm mutant of ETEC H10407, which was designed ETEC/dLT-B (Table 1).

2.3. Cloning and expression of stx2 genes

For expressions of *stx2A* and *stx2AB* operon DNA in JM109, DNA fragments encoding *stx2A* and *stx2AB* operon were cloned into pBAD24 digested with *Kpn*I and *Sph*I, respectively. High-fidelity PCR was carried out with genomic DNA template of Sakai O157 *E. coli* to amplify the *stx2A* and *stx2AB* inserts. An approximately 994-bp amplicon of *stx2A* was generated by PCR with primers VT2-A2-KpnF (GTATAT*GGTACC*GTGTA-TATTATTTAAATGG) and VT2-A2-SphR (CCATAAA*GCATGC*TTCTT-CATGCTTAACTCC), and ~1280-bp amplicon of *stx2AB* operon DNA was obtained from PCR with the common forward primer (VT2-A2-KpnF) and a new reverse primer VT2B-SphR (ACACTTGTTACCC*GCATGC*CAC-GAATCAGG). The resulting pBAD24-derived plasmids carrying the *stx2A* and *stx2AB* operon DNA were named pBAD-*stx2A* and pBAD-*stx2AB*, respectively.

Similarly, for expression of *stx2A1* DNA encoding the A1-fragment of STx2A (processed residues from Arg1 to Arg250) in JM109, the insert DNA was cloned into pBAD24 digested with *Kpn*I and *Sph*I. An approximately 835-bp amplicon of *stx2A1* DNA was generated by PCR with primers VT2-A2-KpnF (common forward primer) and VT2-A1-SphR (CTCTTCATTCAC*GCATGC*TCAGCGAACAGAACGCGC) carrying the restriction site underlined. The resulting pBAD24-derived plasmids carrying the *stx2A1* DNA was named pBAD-*stx2A1*.

E. coli JM109 transformed with the pBAD24-based clone (pBAD-*stx2A*, pBAD-*stx2AB*, and pBAD-*stx2A1*) was cultured in LB-Amp broth until A_{600} (O.D.) reached 0.7, then 0.2% (final conc.) of L-arabinose was added to induce expression of the cloned DNA, and the culture was further incubated for 3 h in a shaker at 37 °C.

2.4. Complementation of STx2A instability with the cloned stxB genes

For the complementation of JM109/pBAD-*stx2A*, pACYC184-derived plasmids pAY-*stx1B* and pAY-*stx2B* were constructed (Table 1). Briefly, DNA fragments encoding *stx1B* and *stx2B* gene were amplified by PCR with genomic DNA template of Sakai O157 *E. coli*. An approximately 330-bp amplicon of *stx1B* was generated by PCR with primers ST1B-BamF (TCT*GGATCC*GCAGAACTATTAGCAG) and ST1B-SalR (CCTGCTATTT*GTCGAC*TGAGCTATTC), and ~320-bp amplicon of *stx2B* DNA was obtained from PCR with primers ST2B-BamF (GGGTAAA-TAAA*GGATCC*GTTAAGCATG) and ST2B-SalR (CACATACCACGAA*GTC-GAC*GGTTATGCCTC). The *stxB* DNA digested with *Bam*HI and *Sal*I was then inserted into pACYC184 digested with same restriction enzymes. The resulting *stxB* clones (named pAY-*stx1B* and pAY-*stx2B*) were designed to be expressed constitutively under the pACYC184-based promoter in the JM109/pBAD-*stx2A* host strain. Similarly, for

complementation of JM109/pBAD-*stx2A1*, pAY-*stx2B* was introduced to be expressed constitutively under the pACYC184-based promoter in the JM109/pBAD-*stx2A1* strain.

2.5. Preparation of periplasmic protein extracts (PPE) and OMVs

The PPE sample was prepared as described in the manual for the PeriPreps™ Periplasting kit (Epicentre®). Briefly, bacterial cells grown overnight were centrifuged (12,000×*g* for 10 min) to discard the culture supernatant. The pellet was resuspended in 0.5 ml of periplasting buffer containing lysozyme and the sample was incubated on ice for 5 min. After osmotic shock for 5 min by adding 0.5 ml of ice-cold purified water, the sample was centrifuged at 12,000×*g* for 5 min to remove the spheroplasts and intact cells from the supernatant. The supernatant recovered was used as PPE.

OMVs were prepared as described previously [17] with slight modifications. Briefly, *E. coli* O157:H7 and its isogenic mutants were inoculated into 500 ml of LB broth and cultured overnight at 37 °C in a shaker. The bacteria were then pelleted by centrifugation (12,000×*g*) for 10 min at 4 °C. The resulting supernatant was recovered and further passed through a 0.22 μm pore-size filter. The OMVs were harvested by concentrating the filterates by using QuixStand™ ultra-filtration system (GE Healthcare) equipped with a membrane cartridge (~100 kDa cutoff size). Then, OMVs in the concentrated sample were collected in the pellet by ultracentrifugation at 100,000×*g* for 2 h at 4 °C. The crude OMV-pellet was resuspended in 3 ml of phosphate buffered saline (PBS, pH7.4) for further OMV purification using sucrose-gradient ultracentrifugation.

2.6. Separation of STx2 subunits and proteolytic susceptibility of STx2A

The A and B subunits of purified STx2 holotoxin (Toxin Technology Inc., USA) were separated by incubation of the toxin in 1 ml of a subunit dissociating solution (6 M urea, 0.1 M NaCl, 0.1 M propionic acid, pH4.0) without stirring at 4 °C for 1 h, as described previously [19]. Then, the toxin preparation was subjected to FPLC (BioRad, Hercules, CA) equipped with Superdex™ 75 column (GE Healthcare, Uppsala, Sweden) to fractionate the A and B subunits. The pooled fractions corresponding to the holotoxin and the STx2A subunit were then freeze-dried and the toxin preparations were suspended in PBS (pH7.4) to be tested for proteolytic susceptibility. Subsequently, the holotoxin and the free STx2A subunit were mixed with the PPE sample of *E. coli* JM109, which was used as a source of periplasmic proteases. After the co-incubation for 5 min at 37 °C, the sample was immediately mixed with SDS-sample buffer prior to boiling for 5 min at 100 °C.

2.7. Immuno-blot (IB) analysis

Protein concentrations of PPE and OMV samples were estimated by using the BCA protein assay kit (Pierce®) and analyzed by SDS-PAGE (15% gel). The separated protein bands were blotted onto nitrocellulose membrane (Invitrogen, USA) for IB analysis. Monoclonal antibodies (mAbs) against bacterial alkaline phosphatase (BAP-77), STx1B (13C4), STx2A (11E10), and LT-A were purchased from various commercial sources. The peroxidase-conjugated rabbit anti-mouse IgG (Sigma, USA) was used as secondary antibody for the enhanced chemiluminescence (ECL) detection of the target proteins.

2.8. Negative staining for transmission electron microscopy (TEM)

To visualize the OMVs, samples were applied to a formvar-coated grid by adsorption. The grid was then stained with 2% uranyl acetate, blotted with filter paper, and then air dried. The samples were examined under a CM20 TEM (Philips, the Netherlands).

3. Results

3.1. Absence of STxA in the periplasm of STxB-deficient mutants

It was previously reported that OMVs of Sakai O157 *E. coli* carry the STx toxins [14], as well as the STxB pentamers in the case of STxA-deficient mutant [7]. In an initial effort to produce the OMVs containing free STxA (uncoupled from STxB), we created a Δ*stx1B* or Δ*stx2B* mutant and the double *stxB* deletion mutant in Sakai O157 *E. coli*. Subsequently, OMVs secreted from the *stxB* mutants were isolated and identified by TEM visualization (Fig. 1A). A TEM image of the OMVs from the *stxB* mutants showed a typical morphology and sizes ranging 20–100 nm in diameter (Fig. 1A), which was not significantly different from those observed previously in *E. coli* O157: H7 [7,17]. To test whether STxA is enclosed within the OMVs, immunoblotting (IB) was performed with anti-STx2A mAb available commercially (clone 11E10, SantaCruz Biotech). Normally STx2A subunit was present in the PPE and OMV samples of the parental (control) Sakai O157 strains (Fig. 1B). However, STx2A was only identified in the STx1B-deficient mutants (lanes 1 and 3, Fig. 1C) but absent in the STx2B-deficient mutants (lanes 2 and 4, Fig. 1C). These results suggest that the toxin A subunit can exist in the periplasm of Sakai O157 *E. coli*, only when coupled to its cognate B-pentamer. Consequently, STx2A was not detected in the OMVs of DM/Δ*stx1B*/ Δ*stx2B* mutant (lane 2, Fig. 1D), compared to the parental strain as positive control (lane 1). These results clearly showed that extracellular secretion of STx2 toxin (possibly STx1; not tested by IB due to lack of commercially available anti-STx1A mAb) can be prevented in the O157 *E. coli* by deficiency of the toxin B subunit. Interestingly, STx2A was not detected by IB in the periplasm (lanes 2 and 4, Fig. 1C), in spite of the presence of STx1B subunit which remained intact in the Δ*stx2B* mutant (lane 1, Fig. 1E).

3.2. Neither transcriptional impairment of the stxA gene nor DegP protease activity was involved in the instability of STxA in the periplasm

To exclude the possibility that instability of STxA in the periplasm of *stxB* mutants (Fig. 1C) might be due to impairment of *stxA* gene transcription, a reverse transcriptase (RT)-PCR was conducted to verify whether transcription of *stxA* genes can occur in the Δ*stxB* mutants of *E. coli* O157:H7. RT-PCR showed that *stxA* gene transcription was not altered in the Δ*stxB* mutants, compared with wild type strain (data not shown). Accordingly, it is unlikely that the absence of STxA in the periplasm is simply associated with the impaired *stxA* gene transcription which might occur due to the *stxB* gene mutation in the *stxAB* operon.

Next, we tested whether DegP would be involved in the possible degradation of the orphan STxA subunit in the STxB-deficient mutant, since DegP has been known to play an important role in the periplasm as a protease, with a broad spectrum of substrates including peri-plasmic and misfolded OM proteins [20,21]. In the IB analysis (Fig. 2A), however, the STx2A was still not rescued in the PPE prepared from the Δ*degP*::Cm mutant of WT/Δ*stx2B*

strain (lane 3, Fig. 2A), compared to the positive (lane 1) and negative (lane 2) controls. The fact that DegP inactivation (lane 3, Fig. 2A) did not rescue the STx2A band in the Δ*stx2B* background may imply that DegP is not involved in the instability of STx2A in the periplasm.

3.3. Absence of LT-A in the periplasm of LT-B-deficient mutant

Since we have shown that STxA is unable to exist in the periplasm in the absence of STxB, we tried to test the possibility that such instability of toxin A subunit in the absence of the B subunit might be a common phenomenon, at least in the context of the AB_5 enterotoxins. Accordingly, a Δ*lt-B*::Cm mutant of ETEC H10407 was created for parallel comparison with the STx case. As shown in Fig. 2B, the LT-A subunit (~28 kDa band) was absent in the PPE sample of the LT-B-deficient mutant (ETEC/dLT-B) when analyzed by IB with anti-LT-A mAb. Therefore, it is likely that the LT-B subunit also could provide a protective role for the LT-A in the periplasm. Because of the similar nature of cholera toxin (CT) and LT [22], one can speculate that CT-A subunit is likely to be unstable in the periplasm of CT-B-deficient mutant of *Vibrio cholera*. However, we did not test this possibility in the present study.

3.4. Complementation of STx2A instability in the periplasm of non-STEC E. coli

To assess the STx2A instability in the periplasm of *E. coli* JM109 strain, a non-STEC background, recombinant plasmids carrying the *stx2A* and *stx2AB* operon DNA (named pBAD-*stx2A* and pBAD-*stx2AB*, respectively) were constructed on the basis of pBAD24 vector [23], and expression of the cloned DNA was induced by L-arabinose addition into the culture of JM109 transformed with the plasmid. Then, IB analysis was carried out with the PPE samples prepared from the JM109 transformants. Consistently, STx2A band was detected in the pBAD-*stx2AB* transformant (lane 2, Fig. 3A) but not in the case with pBAD-*stx2A* (lane 1). This result validates the requirement of the B subunit for the periplasmic presence of STx2A in non-STEC *E. coli*. In order for the complementation of JM109/pBAD-*stx2A*, pACYC184-derived plasmids pAY-*stx1B* and pAY-*stx2B* were constructed for their carriage of the *stx1B* and *stx2B* gene, respectively. The *stxB* clones were designed to be expressed constitutively under the pACYC184-based promoter in the JM109/pBAD-*stx2A* host strain. Interestingly, the arabinose-induced STx2A band was strongly detected in the complementation with either pAY-*stx2B* or pAY-*stx1B* (Fig. 3B), whereas the STx2A expressed in the JM109/pBAD-*stx2A* control strain was hardly detectable by IB (lane 1, Fig. 3B). These results reconfirmed that STxB could play a crucial role for maintaining the stability of STxA during the holotoxin formation in the periplasm.

The crystal structure of the holotoxin [2] reveals that the A2 fragment of STx2A is crucial for interactions with residues in the central pore of the B-pentamer. The pBAD-*stx2A1* clone was thereby constructed to test the assumption that STx2A1 lacking the A2 tail (residues from Ala251 to Lys297) can be expressed independently of the B-pentamer. Interestingly, the A1 fragment (residues from Arg1 to Arg250) can exist alone in the periplasm of JM109, albeit at reduced amount (lane 4, Fig. 3C) when compared to the A1 fragment complemented with STx2B (lane 5, Fig. 3C).

3.5. Instability of STx2A caused by STx2B deficiency is associated with increased proteolytic susceptibility

Next, proteolytic susceptibility to periplasmic proteases was assessed with the free STx2A separated from the purified holotoxin (Toxin Technology Inc., USA), under the assumption that the toxin B subunit may play a role in the protection of the A subunit in the periplasm. Separation of STx2 subunits was conducted as described previously [19]. The elution peak for STx2 holotoxin was evident in faction number 11 as shown in the panel A of Fig. 4 (indicated by AB_5). The inset showed STx2-A and -B subunits separated by SDS-PAGE. The peak for free STx2A (dissociated) appearing around fraction number 14 was collected by HPLC fractionation (panel B, Fig. 4). Accordingly, the free A subunit obtained (Fig. 4B) and STx2 holotoxin were tested for in vitro proteolytic susceptibility toward periplasmic proteases that were provided by the PPE of JM109. A densitometry analysis of the IB results (Fig. 4C) revealed that intensity of STx2A band was 2.2-fold reduced after 5 min co-incubation with the PPE (10 μg) of JM109 at 37 °C. The STx2A band was not detected by IB after 10 min incubation with the source of periplasmic proteases although the holotoxin remained intact after the co-incubation. These results strongly support that the instability of toxin A subunit caused by deficiency of the B subunit might be due to increased susceptibility to the periplasmic proteases.

4. Discussion

Previously, role(s) of toxin B subunits of AB_5 enterotoxins have been largely focused on the ability of binding to cellular receptors [19,24,25], which triggers uptake of the toxin by endocytosis. Because the target substrate of STxA activity (rRNA *N*-glycosidase) is located in the cellular cytosolic compartment, the toxin has to be delivered to the ribosomal site via retrograde intracellular trafficking after internalization 3]. According to the detailed structure of STx2 [2], the A2 fragment serves as a linker domain, tethering the enzymatic A1 fragment to the B-pentamer, as shown in Fig. 5A. The 32 kDa STx2A subunit, subdivided as A1 (yellow) and A2 (magenta) fragments, is known to be non-covalently associated with five STx2B (7.7-kDa) subunits (green). In the absence of the B-pentamer (panel B), the A2-domain (magenta) of STx2A would be then exposed to periplasmic proteases. However, it is uncertain that the C-terminal A2-tail (magenta) of STx2A can be folded correctly or not in the absence of STx2B subunits.

In the case of STx2B deficiency, in this study, the free STx2A then exposes the A2 fragment which remains uncovered in the periplasm, otherwise the alpha-helical portion of the A2 fragment can be securely shielded within the central pore of the B-pentamer (Fig. 5). Also, the upper region above the pore-penetrating alpha-helix portion of the A2 fragment might be inaccessible because of tight association at the interface between the A1-fragment and the B-pentamer. Although the toxin B-subunit forms a stable pentameric structure [7,25,26], the toxin A subunit alone was highly unstable in the periplasm as shown in this study. Therefore, it was of interest to determine whether site-specific deletion of the A2 tail in the STxA could stabilize the truncated A subunit in the periplasm in the absence of STxB. As shown in Fig. 3C, the truncated STx2A protein lacking the A2 tail can exist alone in the periplasm of JM109, albeit at reduced amount (lane 4) compared to the A1 fragment complemented with

STx2B (lane 5). Interestingly, stability of the A1 fragment was increased in the periplasm when complemented with STx2B (lane 5), indicating that the A1 fragment can still interact with the B-pentamer. These results suggest that the A2 fragment in the absence of the B-pentamer might be partially misfolded and thus slowly targeted towards the periplasmic proteases. However, the exposure of the A2 fragment in the absence of STxB (panel B, Fig. 5) appears to render the A subunit highly susceptible to periplasmic proteases.

In vitro, STx holotoxin hybrids (for example; VT1A:VT2B and VT2A:VT1B) can be assembled with the purified dissociated subunits [19]. Although, STx2A:STx1B hybrid formation was identified in K-12 *E. coli* host carrying the plasmid clones, in vivo formation of STx1A: STx2B hybrid was not detected in the previous reports [27,28]. Accordingly, formation of STx2A:STx1B hybrid can be possible in the *stx2B* mutant of Sakai O157 stain in which *stx2A* and *stx1B* genes remain intact. However, as shown in Fig. 1C, such a hetero-subunit hybrid toxin was not detected in the periplasm of Sakai O157 mutants, but in the complementation of the JM109/pBAD-*stx2A* strain with pAY-*stx1B* plasmid the STx2A was stably present in the periplasm (Fig. 3B). Although the hybrid (STx2A:STx1B) toxin was not detected in the Δ*stx2B* mutant of Sakai O157 strain, it can be formed in the JM109 host as inferred from the complementation experiment (Fig. 3B). We reasoned that STx1B would have a higher likelihood to combine with the STx1A rather than STx2A in the Δ*stx2B* mutant, so that the subsequent binding of STx1B to STx2A and its role proposed for the protection of the A subunit from proteolysis (Fig. 4) are unlikely in the case of Sakai Δ*stx2B* mutant. It will be interesting to test whether the STx2A:STx1B hybrid can be detected or not in the Δ*stx2B*/Δ*stx1A* mutant of Sakai O157 *E. coli*.

In this study, we tried to understand why the toxin A subunits are unable to exist alone in the periplasm of the B subunit-deficient mutants. One explanation is that susceptibility of the free A subunit towards periplasmic proteases was increased, as shown in Fig. 4. In the *E. coli* periplasm, a number of proteases have been identified including DegP [29,30]. Since DegP is an important periplasmic protease with a broad spectrum of substrates, including periplasmic and misfolded OM proteins [20,21], we tested the possible involvement of DegP in the instability of the free toxin A subunit. However, such instability of toxin A subunit is not simply associated with DegP (Fig. 2A) or impairment of *stxA* gene transcription in the *stxB* mutants. Further study would be required to elucidate the mechanism underlying proteolysis of the free A subunit in the periplasm and the exact role of toxin B subunit involved in the stability of the A subunit during the holotoxin assembly.

In conclusion, we have shown that the toxin B subunits (in both STx and LT) are required for the stability of the A subunit during the AB_5 toxin assembly in the bacterial periplasm. To our best knowledge, these observations would be the first report showing that such instability of toxin A subunit in the absence of its cognate B subunit is a common phenomenon in the closely related AB_5 bacterial toxins and that the toxin B subunit plays an essential role in stabilizing the A subunit during the AB_5 toxin assembly in the bacterial periplasm. Since the OMVs of STxB-deficient mutants were not cytotoxic to Vero cells (data not shown), target inactivation of the toxin B-subunit would provide a new approach towards detoxification of OMVs from diverse pathogenic bacteria capable of producing AB_5 toxins.

Acknowledgments

This study was supported by grants from KRIBB Research Initiative Program (KBM4311022), and from the Technology Development Program (AGM0501012) for Agriculture and Forestry, Republic of Korea. Work in the laboratory of REB was supported by CIHR Operating Grant MOP-84329.

References

1. Paton JC, Paton AW. Pathogenesis and diagnosis of Shiga toxin-producing *Escherichia coli* infections. Clin Microbiol Rev. 1998; 11:450–479. [PubMed: 9665978]
2. Fraser ME, Fujinaga M, Cherney MM, et al. Structure of Shiga toxin type 2 (Stx2) from *Escherichia coli* O157:H7. J Biol Chem. 2004; 279:27511–27517. [PubMed: 15075327]
3. Johannes L, Römer W. Shiga toxins — from cell biology to biomedical applications. Nat Rev Microbiol. 2010; 8:105–116. [PubMed: 20023663]
4. Endo Y, Tsurugi K, Yutsudo T, et al. Site of action of a Vero toxin (VT2) from *Escherichia coli* O157:H7 and of Shiga toxin on eukaryotic ribosomes. RNA *N*-glycosidase activity of the toxins. Eur J Biochem. 1988; 171:45–50. [PubMed: 3276522]
5. Lingwood CA. Role of verotoxin receptors in pathogenesis. Trends Microbiol. 1996; 4:147–153. [PubMed: 8728608]
6. Donohue-Rolfe A, Jacewicz M, Keusch GT. Isolation and characterization of functional Shiga toxin subunits and renatured holotoxin. Mol Microbiol. 1989; 3:1231–1236. [PubMed: 2677606]
7. Kim SH, Lee SR, Kim KS, et al. Shiga toxin A subunit mutant of *Escherichia coli* O157:H7 releases outer membrane vesicles containing the B-pentameric complex. FEMS Immunol Med Microbiol. 2010; 58:412–420. [PubMed: 20199568]
8. Hayashi T, Makino K, Ohnishi M, et al. Complete genome sequence of enterohemorrhagic *Escherichia coli* O157:H7 and genomic comparison with a laboratory strain K-12. DNA Res. 2001; 8:11–22. [PubMed: 11258796]
9. Tarr PI, Gordon CA, Chandler WL. Shiga-toxin-producing *Escherichia coli* and haemolytic uraemic syndrome. Lancet. 2005; 365:1073–1086. [PubMed: 15781103]
10. Hirst TR, Sanchez J, Kaper JB, et al. Mechanism of toxin secretion by *Vibrio cholerae* investigated in strains harbouring plasmids that encode heat-labile enterotoxins of *Escherichia coli*. Proc Natl Acad Sci U S A. 1984; 81:7752–7756. [PubMed: 6393126]
11. Tauschek M, Gorrell RJ, Strugnell RA, et al. Identification of a protein secretory pathway for the secretion of heat-labile enterotoxin by an enterotoxigenic strain of *Escherichia coli*. Proc Natl Acad Sci U S A. 2002; 99:7066–7071. [PubMed: 12011463]
12. Kato S, Kowashi Y, Demuth DR. Outer membrane-like vesicles secreted by *Actinobacillus actinomycetemcomitans* are enriched in leukotoxin. Microb Pathog. 2002; 32:1–13. [PubMed: 11782116]
13. Kuehn MJ, Kesty NC. Bacterial outer membrane vesicles and the host pathogen interaction. Genes Dev. 2005; 19:2645–2655. [PubMed: 16291643]
14. Kolling GL, Matthews KR. Export of virulence genes and Shiga toxin by membrane vesicles of *Escherichia coli* O157:H7. Appl Environ Microbiol. 1999; 65:1843–1848. [PubMed: 10223967]
15. Horstman AL, Kuehn MJ. Enterotoxigenic *Escherichia coli* secretes active heat-labile enterotoxin via outer membrane vesicles. J Biol Chem. 2000; 275:12489–12496. [PubMed: 10777535]
16. Horstman AL, Bauman SJ, Kuehn MJ. Lipopolysaccharide 3-deoxy-D-manno-octulosonic acid (Kdo) core determines bacterial association of secreted toxins. J Biol Chem. 2004; 279:8070–8075. [PubMed: 14660669]
17. Kim SH, Kim KS, Lee SR, et al. Structural modifications of outer membrane vesicles to refine them as vaccine delivery vehicles. Biochim Biophys Acta. 2009; 1788:2150–2159. [PubMed: 19695218]
18. Datsenko KA, Wanner BL. One-step inactivation of chromosomal genes in *Escherichia coli* K-12 using PCR products. Proc Natl Acad Sci U S A. 2000; 97:6640–6645. [PubMed: 10829079]

19. Head SC, Karmali MA, Lingwood CA. Preparation of VT1 and VT2 hybrid toxins from their purified dissociated subunits. Evidence for B subunit modulation of A subunit function. J Biol Chem. 1991; 266:3617–3621. [PubMed: 1847382]

20. Spiess C, Beil A, Ehrmann M. A temperature-dependent switch from chaperone to protease in a widely conserved heat shock protein. Cell. 1999; 97:339–347. [PubMed: 10319814]

21. Clausen T, Southan C, Ehrmann M. The HtrA family of proteases: implications for protein composition and cell fate. Mol Cell. 2002; 10:443–455. [PubMed: 12408815]

22. Neill RJ, Ivins BE, Holmes RK. Synthesis and secretion of the plasmid-coded heat-labile enterotoxin of *Escherichia coli* in *Vibrio cholerae*. Science. 1983; 221:289–291. [PubMed: 6857285]

23. Guzman LM, Belin D, Carson MJ, et al. Tight regulation, modulation, and high-level expression by vectors containing the arabinose P_{BAD} promoter. J Bacteriol. 1995; 177:4121–4130. [PubMed: 7608087]

24. Lindberg AA, Brown JE, Stromberg N, et al. Identification of the carbohydrate receptor for Shiga toxin produced by *Shigella dysenteriae* type 1. J Biol Chem. 1987; 262:1779–1785. [PubMed: 3543013]

25. Pina DG, Johannes L. Cholera and Shiga toxin B-subunits: thermodynamic and structural considerations for function and biomedical applications. Toxicon. 2005; 45:389–393. [PubMed: 15733559]

26. Williams JP, Green BN, Smith DC, et al. Noncovalent Shiga-like toxin assemblies: characterization by means of mass spectrometry and tandem mass spectrometry. Biochemistry. 2005; 44:8282–8290. [PubMed: 15938618]

27. Weinstein DL, Jackson MP, Perera LP, et al. In vivo formation of hybrid toxins comprising Shiga toxin and the Shiga-like toxins and role of the B subunit in localization and cytotoxic activity. Infect Immun. 1989; 57:3743–3750. [PubMed: 2807546]

28. Smith MJ, Teel LD, Carvalho HM, et al. Development of a hybrid Shiga holotoxoid vaccine to elicit heterologous protection against Shiga toxin types 1 and 2. Vaccine. 2006; 24:4122–4129. [PubMed: 16551486]

29. Wulfing C, Pluckthun A. Protein folding in the periplasm of *Escherichia coli*. Mol Microbiol. 1994; 12:685–692. [PubMed: 8052121]

30. Miot M, Betton JM. Protein quality control in the bacterial periplasm. Microb Cell Fact. 2004; 3:4. [PubMed: 15132751]

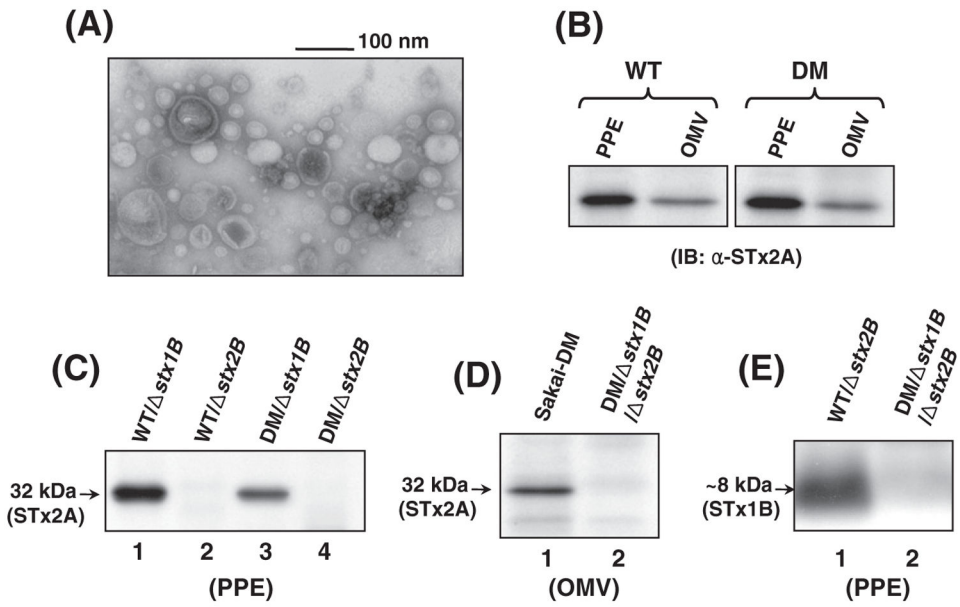

Fig. 1.

TEM and IB analyses for characterization of the Δ*stxB* mutants. (A) TEM visualization of OMVs from Sakai-DM/Δ*stx2B* mutant. The image showed typical sizes of OMVs ranges 20–100 nm in diameter. (B, C, and D) Immunoblots for detection of STx2A subunit in the PPE and OMV samples. STx2A was identified in the periplasm and OMVs of the parental O157 strains (B) by using anti-STx2A mAb, however, it was absent in the PPE samples (lanes 2 and 4, C) and the OMVs (lane 2, D) of the Δ*stx2B* mutants. (E) STx1B subunit was probed with anti-STx1B mAb in the periplasm of the Δ*stx2B* mutant (lane 1) but was absent in the Δ*stx1B* mutant (lane 2).

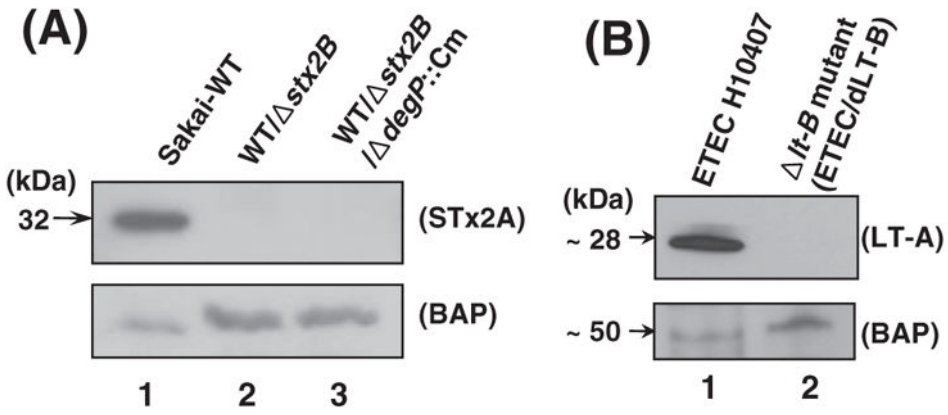

Fig. 2.

IB analysis of periplasmic proteins extracted from STEC and ETEC mutants. (A) The STx2A subunit was detected in the PPE samples of STEC O157 Sakai derivatives. STx2A band was present only in the wild type strain (lane 1) but absent in the both Δ*stx2B* and Δ*stx2B*/Δ*degP*::Cm mutants (lanes 2 and 3, respectively). Inactivation of *degP* in the Δ*stx2B* mutant background did not rescue the STx2A band in the periplasm (lane 3), suggesting that DegP might be not associated with the absence of STx2A. BAP (bacterial alkaline phosphatase as a periplasmic protein marker) was used as an internal control for the PPE samples. (B) PPE samples of ETEC H10407 and its LT-B-deficient mutant (ETEC/dLT-B) were analyzed by using anti-LT-A mAb (Abcam). As shown, the LT-A subunit (~28 kDa band) was absent in the Δ*lt-B* mutant (lane 2), compared to wild type strain (lane 1).

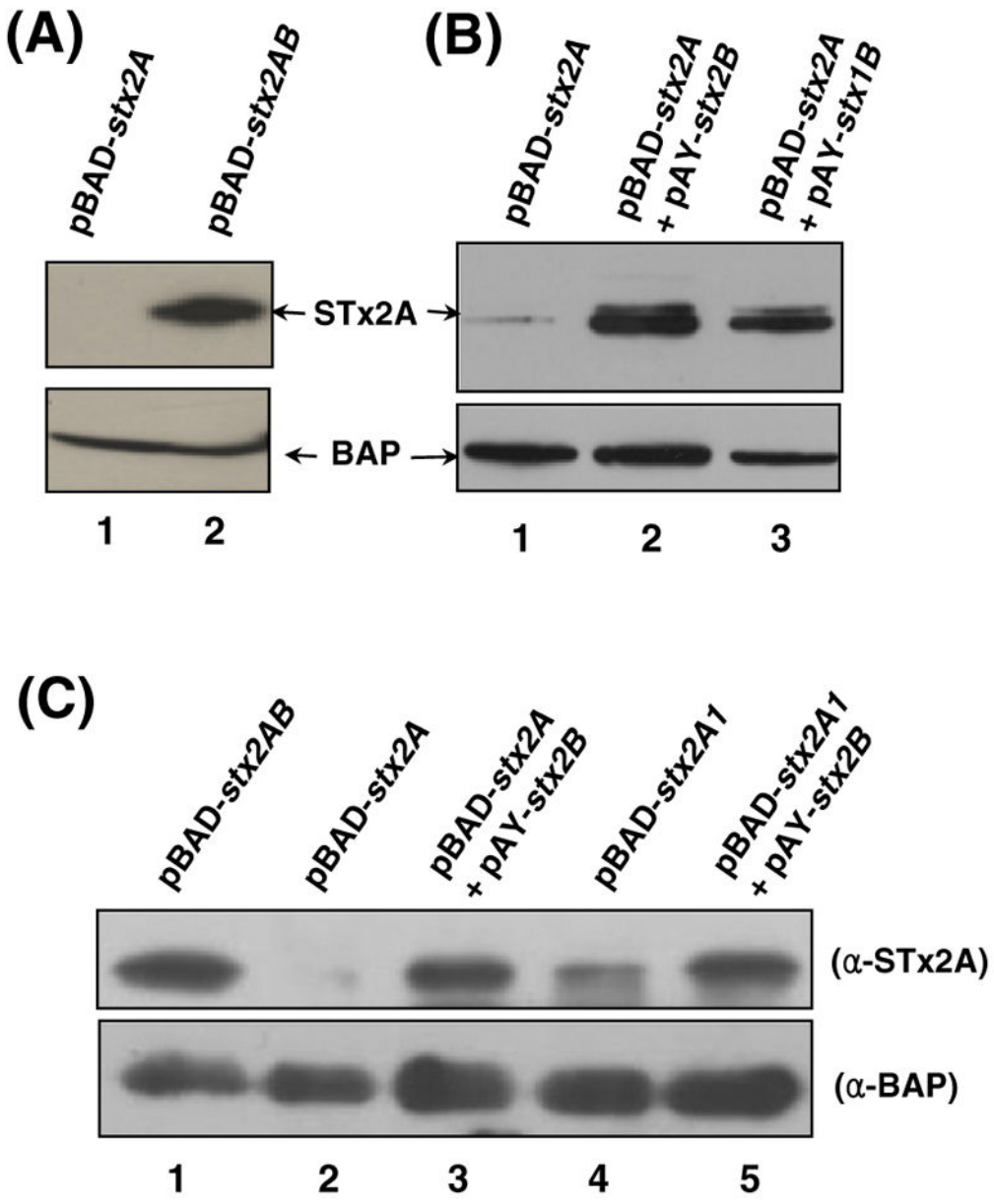

Fig. 3.

IB analysis of PPE samples of JM109 transformants. (A) PPE samples prepared from the JM109 cells harboring the respective pBAD-*stx2A* and pBAD-*stx2AB* clone were immunoblotted with anti-STx2A mAb. (B) For the complementation of JM109/pBAD-*stx2A*, plasmid pAY-*stx1B* or pAY-*stx2B* was introduced. STx2A band was strongly detected in the complementation with either pAY-*stx2B* or pAY-*stx1B*, whereas STx2A subunit overexpressed in the JM109/pBAD-*stx2A* strain (lane 1) was hardly detectable by IB with anti-STx2A mAb. (C) IB was performed to see whether A1 fragment of STx2A can exist alone in the periplasm of JM109. PPE of JM109/pBAD-*stx2A1* contained the A1 fragment, albeit at reduced amount (lane 4) compared to the A1 fragment complemented with STx2B (lane 5).

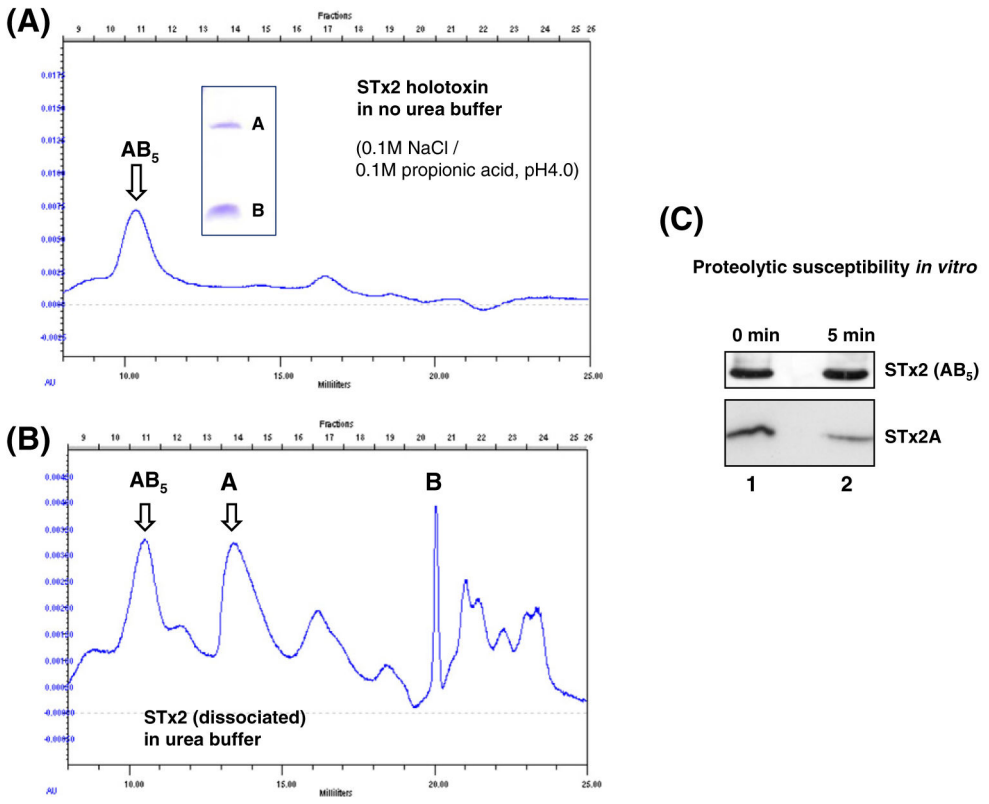

Fig. 4.

In vitro STx2A susceptibility to proteolytic degradation by periplasmic proteases. (A and B) The purified STx2 holotoxin (Toxin Technology Inc., USA) and the free STx2A subunit fractionated by HPLC as described previously [19] were subjected to proteolytic susceptibility assay with the PPE from JM109. The inset (A) showed STx2-A and -B subunit separated by SDS-PAGE. (C) Approximately half of the free STx2A (2.2-fold reduction in the band intensity) was degraded in 5 min co-incubation with the PPE (10 μg) from JM109 at 37 °C, while the holotoxin (5 μg) remained intact after the co-incubation with the source of periplasmic proteases.

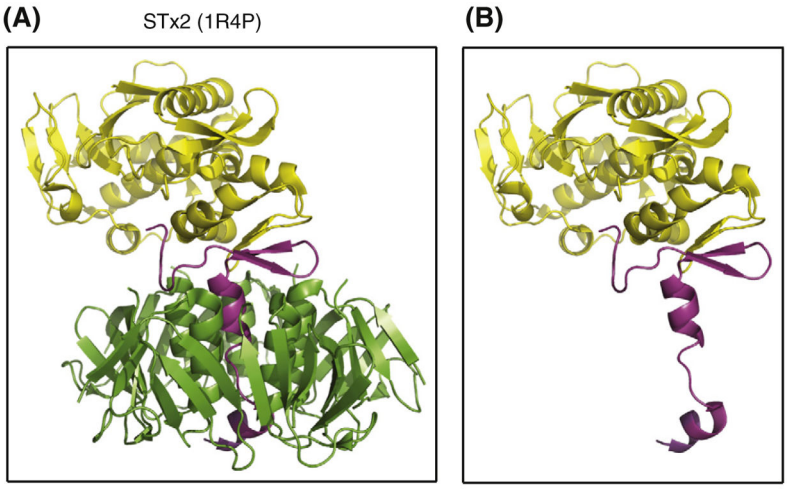

Fig. 5.

Ribbon structure of STx2 toxin. Structures of STx2 holotoxin (A) and STx2A (B) were obtained from the Protein Data Bank (accession code: 1R4P) and displayed after manipulation by using the PyMOL Molecular Graphics System, Version 1.3, Schrödinger, LLC. The 32 kDa STx2A subunit, subdivided as A1 (yellow) and A2 (magenta) fragments in the panel A, is known to be non-covalently associated with five STx2B (7.7-kDa) subunits (green). In the absence of the B-pentamer (panel B), the A2-domain (magenta) of STx2A would be then exposed to periplasmic proteases. (For interpretation of the references to color in this figure legend, the reader is referred to the web version of this article.)

Table 1

Bacterial strains and plasmids used in this study.

Strains/plasmids	Property	Source/Refs.
E. coli O157:H7 strain Sakai	Wild type	[8]
Sakai-DM	Δ*msbB1*/*msbB2* mutant of wild type Sakai strain	This study
DM/Δ*stx1B*	Δ*stx1B* mutant of Sakai-DM	This study
DM/Δ*stx1B*/*stx2B*	Δ*stx1B*/*stx2B*::Cm mutant of Sakai-DM	This study
DM/Δ*stx2A*::Cm	Δ*stx2A*::Cm mutant of Sakai-DM	[7]
WT/Δ*stx1B*	Δ*stx1B* mutant of Sakai wild type (WT)	This study
WT/Δ*stx2B*	Δ*stx2B* mutant of Sakai-WT	This study
WT/Δ*stx2B*/Δ*degP*	Δ*degP*::Cm mutant of Sakai-WT/Δ*stx2B*	This study
ETEC H10407	A reference strain of enterotoxigenic *E. coli* (LT^+)	Lab collection
ETEC/dLT-B	Δ*lt-B*::Cm mutant of ETEC H10407	This study
E. coli JM109	*endA1 gyrA96 thi hsdR17 supE44 relA1 traD36* Δ (*lac-proAB*)/F′ (*proAB lacI*^{q}*Z* M15)	Lab collection
pKD46	A ***t***^{S}-plasmid encoding arabinose-inducible λ-Red recombinase (Amp^R)	[18]
pKD3	A template plasmid carrying the FRT-Cm-FRT cassette (Cm^R)	[18]
pCP20	A ***t***^{S}-plasmid encoding the FLP recombinase (Amp^R/Cm^R)	[18]
pSTx1B::Cm	pUC18-based recombinant plasmid carrying the Δ*stx1B*::Cm allele (Cm^R/Amp^R)	This study
pSTx2B::Cm	pUC18-based recombinant plasmid carrying the Δ*stx2B*::Cm allele (Cm^R/Amp^R)	This study
pDegP::Cm	pUC18-based recombinant plasmid carrying the Δ*degP*::Cm allele (Cm^R/Amp^R)	This study
pUC18	General cloning vector (Amp^R)	Lab collection
pACYC184	General cloning vector (Cm^R), p15A (*rep*) origin	Lab collection
pAY-*stx1B*	pACYC184-based recombinant plasmid carrying the *stx1B* gene (Cm^R)	This study
pAY-*stx2B*	pACYC184-based recombinant plasmid carrying the *stx2B* gene (Cm^R)	This study
pBAD24	An arabinose-inducible expression vector (Amp^R), pBR322 (pMB1 *rep*) origin	[23]
pBAD-*stx2A*	pBAD24-based recombinant plasmid carrying the *stx2A* gene (Amp^R)	This study
pBAD-*stx2AB*	pBAD24-based recombinant plasmid carrying the *stx2AB* operon (Amp^R)	This study
pBAD-*stx2A1*	pBAD24-based recombinant plasmid carrying the *stx2A1* allele (Amp^R)	This study